Monthly Notices
of the
ROYAL ASTRONOMICAL SOCIETY
MNRAS **455,** 2279–2288 (2016) doi:10.1093/mnras/stv2430

On the Erigone family and the z_2 secular resonance

V. Carruba,[1,2]★ S. Aljbaae[1]★ and O. C. Winter[1]★

[1]*Grupo de dinâmica Orbital e Planetologia, UNESP, Univ. Estadual Paulista, Guaratinguetá SP 12516-410, Brazil*
[2]*Department of Space Studies, Southwest Research Institute, Boulder, CO 80302, USA*

Accepted 2015 October 19. Received 2015 October 19; in original form 2015 August 03

ABSTRACT

The Erigone family is a C-type group in the inner main belt. Its age has been estimated by several researchers to be less then 300 Myr, so it is a relatively young cluster. Yarko-YORP Monte Carlo methods to study the chronology of the Erigone family confirm results obtained by other groups. The Erigone family, however, is also characterized by its interaction with the z_2 secular resonance. While less than 15 per cent of its members are currently in librating states of this resonance, the number of objects, members of the dynamical group, in resonant states is high enough to allow us to use the study of dynamics inside the z_2 resonance to set constraints on the family age. Like the ν_6 and z_1 secular resonances, the z_2 resonance is characterized by one stable equilibrium point at $\sigma = 180^\circ$ in the z_2 resonance plane $(\sigma, \frac{d\sigma}{dt})$, where σ is the resonant angle of the z_2 resonance. Diffusion in this plane occurs on time-scales of $\simeq 12$ Myr, which sets a lower limit on the Erigone family age. Finally, the minimum time needed to reach a steady-state population of z_2 librators is about 90 Myr, which allows us to impose another, independent constraint on the group age.

Key words: celestial mechanics – Minor planets, asteroids: general – Minor planets, asteroids: individual: Erigone.

1 INTRODUCTION

The Erigone family is a C-type group in the inner main belt. Its age has been estimated to be 280^{+30}_{-50} Myr by Vokrouhlický et al. (2006c) with a Yarkovsky and Yarkovsky -O'Keefe -Radzievsky -Paddack (YORP, overall we defined this method as Yarko-Yorp) Monte Carlo approach, 170^{+25}_{-30} Myr by Bottke et al. (2015) with a modified Yarko-Yorp Monte Carlo approach that also includes the effect of stochastic YORP, and as 220^{+60}_{-80} Myr in Spoto, Milani & Knežević (2015). There seems therefore to be a significant consensus in the literature that the Erigone family should be a relatively young C-type cratering family. Much less attention has been given to its secular properties. This group is characterized by its interaction with the z_2 secular resonance (Carruba & Michtchenko 2009), a resonance of the $(2g + s)$-type introduced by Milani & Knežević (1994) using the perturbation theory of Milani & Knežević (1990).[1] About 15 per cent of the current Erigone family members are in librating states of the z_2 secular resonance. While this is not a majority of the members, as for the case of the Tina family and the ν_6 secular resonance (100 per cent, Carruba & Morbidelli 2011), the Agnia and Padua families, with more than 50 per cent of the members in z_1 librating states (Vokrouhlický et al. 2006b; Carruba 2009), dynamics inside the z_2 secular resonance can still be used to obtain estimates, or at least lower limits, of the family age.

Also, dynamics inside the z_2 secular resonance has not so far been given a lot of attention. As for the ν_6 and z_1 secular resonances, we found an equilibrium point in the $(\sigma, \frac{d\sigma}{dt})$ plane at $\sigma = 180^\circ$, where σ is the resonant argument of the z_2 secular resonance. The minimum time needed to fully disperse an originally compact family in this plane fully around the equilibrium point can be used to set constraint on the group age. Furthermore, checking the minimum time needed to inject a steady-state librating population into the z_2 secular resonance can also provide constraints on the Erigone family age of a nature not previously used in the literature.

This paper is so divided: in Section 2, we obtain dynamical maps and synthetic proper elements for asteroids in the orbital region of Erigone. Section 3 deals with secular dynamics in the area. In this section, we estimate the population of likely resonators of the main secular resonances in the region (Carruba 2009), and verified their resonant behaviour by studying their resonant arguments. Section 4 revisits physical properties of the local asteroids such as taxonomy, geometric albedo, and estimated masses. In Section 5, we identify the Erigone family in various domains of proper elements,

★ E-mail: vcarruba@feg.unesp.br (VC); safwanaljbaae@obspm.fr (SA); ocwinter@feg.unesp.br (OCW)

[1] Secular resonances involve commensurabilities between the asteroid proper frequency of precession of argument of pericentre g and longitude of the node s and that of planets. The z_2 secular resonance is a non-linear secular resonance that involves the combination of the two linear resonances $\nu_6 = g - g_6$ and $\nu_{16} = s - s_6$, where the subscript 6 is associated with the sixth planet, Saturn. In particular, $z_2 = 2\nu_6 + \nu_{16} = 2(g - g_6) + (s - s_6)$.

frequency, and photometric colours. In Section 6, we use Yarko-Yorp Monte Carlo method to obtain a preliminary estimate of the family age. In Section 7, we investigate the dynamics inside the z_2 secular resonance and the constraints that it may provide on the age of the Erigone family. Section 8 deals with the dynamical evolution of the Erigone family, simulated with the SYSYCE integrator of Carruba et al. (2015). Minimum times needed to inject into the z_2 secular resonance a steady-state population allowed us to set further constraints on the Erigone family age. Finally, in Section 9, we present our conclusions.

2 PROPER ELEMENTS

To study the local dynamics we first obtained a proper elements map in the region of the Erigone family. We computed synthetic proper elements with the method discussed in Carruba (2010) for a grid of 51 by 75 (i.e., 3825) test particles in the (a, $\sin(i)$) plane. Values of proper i ranged from $3\overset{\circ}{.}80$ to $6\overset{\circ}{.}76$, while values of proper a were in the range from 2.3 to 2.5 au. All the other initial angles and the eccentricity were those of (4) Erigone at J2000.

Results are shown in Fig. 1, where each black dot identifies the proper elements of a given test particle. Mean-motion resonances are shown as vertical red lines in the figure, while secular resonances appear as inclined bands of lower number density of proper elements. We identify all mean-motion resonances up to order 13 and all linear secular resonances (and some non-linear) in the system. The Erigone family is characterized by its interaction with the $z_2 = 2(g - g_6) + s - s_6$ secular resonance, that appears in the map as an inclined band at approximately $a = 2.35$ au. We also plotted as blue circles particles whose value of $2g + s$ is in the range of $2g_6 + s_6 \pm 0.3$ arcsec yr^{-1}, and that are likely to be found in z_2 librating states (see Section 3 for further details). Other non-linear secular resonances in the region are the g −type $3\nu_6 - \nu_5$ resonance and the $g + 2s$-type $\nu_5 + 2\nu_{16}$, plus harmonics involving combination of other planets proper frequencies as Uranus.

We then computed proper elements for numbered objects in the region of the Erigone family, defined as a box in the (a, e, $\sin(i)$) space whose limits are given by the maximum and minimum proper elements of the Erigone family halo, as obtained in Carruba et al. (2013). Of the 4956 asteroids that we integrated, whose osculating elements were downloaded from the AstDyS site (http://hamilton.dm.unipi.it/astdys, Knežević & Milani 2003) on 2014 June 24, all survived a 10 Myr integration. We computed synthetic proper elements, and we eliminated all objects for which one of the proper elements a, e, $\sin(i)$ or proper frequencies g and s had errors larger than those classified as 'pathological' by Knežević & Milani (2003); i.e., $\Delta a = 0.01$ au, $\Delta e = 0.1$, $\Delta\sin(i) = 0.03$, and $\Delta g = \Delta s = 10$ arcsec yr^{-1}. This left us with a data set of 4717 asteroids with good-quality proper elements.

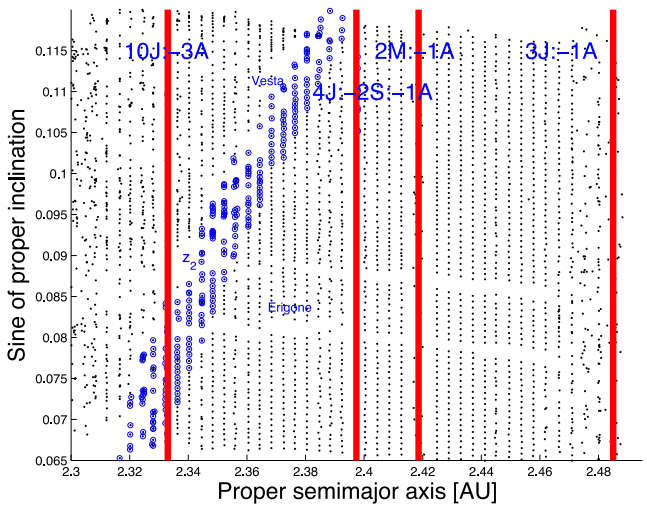

Figure 1. Dynamical map in the proper (a, $\sin(i)$) space for the orbital region of the Erigone family. Vertical red lines display the positions of the main mean-motion resonances, blue circles identify z_2 likely resonators.

The Erigone family appears as a two-lobed structure among asteroids with stable elements. The main sources of instabilities on proper a in the Erigone region are associated with the 10J:-3A, 4J:-2S:-1A and 2M:-1A mean-motion resonances. Other minor three-body and four-body resonances are not shown in Fig. 1 for simplicity. Secular dynamics in the Erigone area will be discussed in the next section.

3 SECULAR DYNAMICS IN THE ERIGONE REGION

Secular resonances occur when there is a commensurability between the proper frequency of precession of the argument of pericentre g or of the longitude of the node s of a given asteroid and a planet. If the commensurability is just between one frequency of the asteroid and one frequency of the planet, such as in the case of the $\nu_6 = g - g_6$ secular resonance, the resonance is linear. Higher order resonances involving more complex combinations of asteroidal and planetary frequencies, such as for instance the $z_1 = \nu_6 + \nu_{16} = g - g_6 + s - s_6$ resonance, are called non-linear secular resonances. Carruba (2009) defines as likely resonators the asteroids whose frequency combination is to within ± 0.3 arcsec yr^{-1} from the resonance centre for the case of the z_1 secular resonance. For the the z_2 resonance, this means that $2g + s = 2g_6 + s_6 = 30.345$ arcsec yr^{-1} (we are using values of the planetary frequencies from Milani & Knežević 1994, see also table 1 in Carruba & Michtchenko 2007). About 90 per cent of the z_1 likely resonators in the Padua family area were found to be actual librators, when the resonant argument of the resonance was analysed (librators were defined as objects whose resonance argument was observed to librate for the whole length of the numerical simulation performed to check their status, i.e. 20 Myr).[2]

Table 1 displays the main secular resonances involving Jupiter and Saturn frequencies in the region labelled in terms of combination of linear resonances and proper frequencies, the values of the asteroid resonant frequencies, the number of likely resonators, and the number of objects for which the resonant argument was actually in libration. Local secular resonances involving Martian frequencies have been discussed in Carruba et al. (2005). Interested readers could find more information in that paper. For simplicity, we do not show in the table resonances involving Uranus frequencies. Since the g_7 frequency is quite close to the g_5, resonances involving g_7 are very close in proper element space to those involving g_5, and of lower strength.

Fig. 2, panel A, displays a (g,2g+s) projection of the 4171 asteroids with known proper elements in our sample. Blue lines identify

[2] Since the resonances studied in this work are of higher order and degree then the z_1, their actual width should be smaller. Using the 0.3 arcsec yr^{-1} criteria could therefore overestimate a bit the number of actual resonators. Yet, since the actual width of a given resonance is difficult to predict before an analysis in (σ, $\frac{d\sigma}{dt}$) plane of each resonance is performed, we believe that using the 0.3 arcsec yr^{-1} should be a reasonable first-order approximation.

Table 1. Main secular resonances in the Erigone region labelled in terms of combination of linear resonances and proper frequencies, frequency value, number of likely and actually resonant asteroids.

Resonance argument in terms of linear resonances	Resonance argument in terms of proper frequencies	Frequency value (arcsec yr^{-1})	Likely resonators	Actual resonators
g resonances				
$3\nu_6 - \nu_5$	$2g - 3g_6 + g_5$	40.236	397	75
g+2s resonances				
$\nu_5 + 2\nu_{16}$	$g + 2s - g_5 - 2s_6$	−48.433	192	38
2g+s resonances				
$z_2 = 2\nu_6 + \nu_{16}$	$2g + s - 2g_6 - s_6$	30.345	493	367

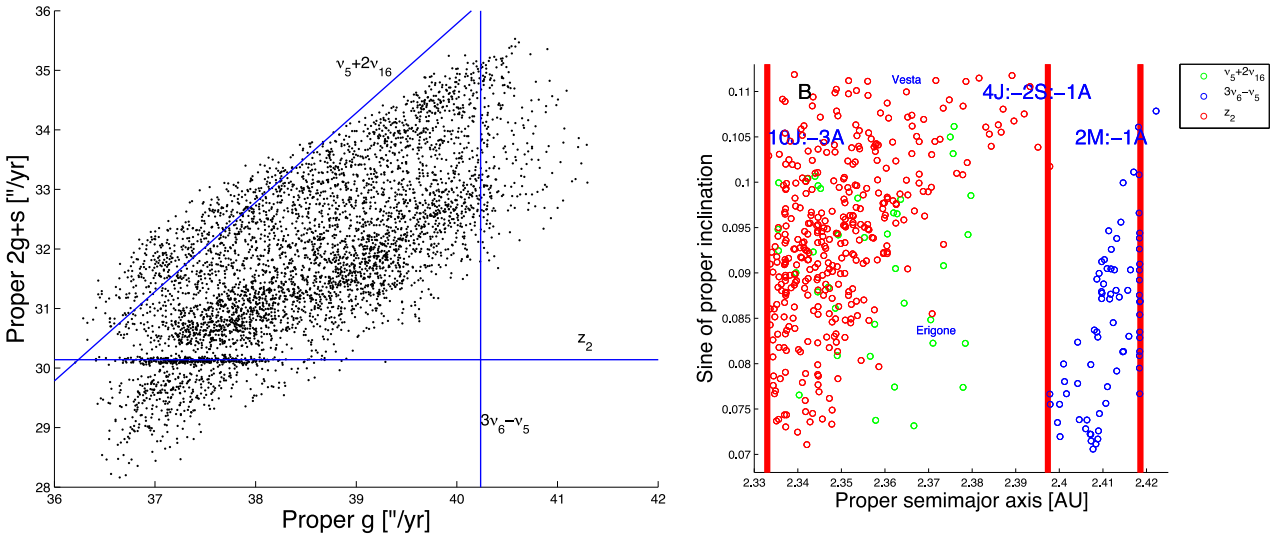

Figure 2. Panel A: a (g,2g+s) projection of the 4171 asteroids with known proper elements in our sample. Blue lines identify the location of the secular resonances listed in Table 1 with a number of 'likely resonators' larger than 1. Panel B: an (a, sin (i)) projection of the actual resonators population listed in Table 1.

the location of the secular resonances listed in Table 1. Note the horizontal alignment of objects along the z_2 secular resonance, suggesting the dynamical importance of this commensurability. Panel B displays an (a, sin (i)) projection of the actual resonators population. Some of the asteroids in $3\nu_6 - \nu_5$ librating states are also inside the 2M:-1A mean-motion resonance, whose dynamics has been studied in Gallardo et al. (2011). Despite all three studied resonances being of order 6, the z_2 resonance plays by far the major role in dispersing asteroids in the Erigone area. This may be caused by the fact that the torsions of the secular resonances, even if associated with terms of the same order, can be different by an order of magnitude (Milani & Knežević 1994). The role of the z_2 resonance in affecting the evolution of members of the Erigone family will be investigated in further detail in later sections. Here, we start by having a closer look at the main frequencies involved in this dynamics.

Fig. 3, panel A, shows the time behaviour of the resonant argument $\sigma = 2(\varpi - \varpi_6) + (\Omega - \Omega_6)$ for (8089) Yukar, the lowest numbered among the z_2 resonant asteroids (black dots). To emphasize the long-time behaviour of the angle and eliminate all short-period perturbations such as the g_5 frequency in the precession of Saturn's pericentre, the argument σ was digitally filtered, so to eliminate all frequencies with period less than 700 000 yr (Carruba et al. 2005). Results are shown as red asterisks.

The reader may notice that there are two main frequencies, one associated with short-period oscillation around the centre of libration, with a period of $\simeq$ 0.06 Myr, and another with oscillations of the centre of libration itself, with a period of $\simeq$ 6.1 Myr. Fig. 3, panel B, shows the orbital evolution in a polar diagram, with axes ($\psi_1{}^S$, $\psi_2{}^S$) defined as

$$\psi_1{}^S = \sqrt{2(1-\sqrt{1-e^2})}\cos\left[2(\varpi - \varpi_6) + (\Omega - \Omega_6)\right], \quad (1)$$

and,

$$\psi_2{}^S = \sqrt{2(1-\sqrt{1-e^2})}\sin\left[2(\varpi - \varpi_6) + (\Omega - \Omega_6)\right], \quad (2)$$

where e is the asteroid eccentricity. Charlier (1902) introduced these variables (which are asymptotically equal to $e\cos\sigma$ and $e\sin\sigma$ for small e) in his theory for secular resonances. Again, black dots show the evolution with orbital elements filtered up to a period of 700 yr, while the curve shows the evolution with elements filtered up to a period of 700 000 yr. The red asterisks describe an arc associated with a banana-shape orbit, visible at higher resolutions than that used for Fig. 3, panel B, with period of about 6.1 Myr, a similar behaviour is shared by other resonant asteroids in the region.

Having examined the effect of local dynamics, we are now ready to analysize the taxonomical properties of asteroids in the Erigone region.

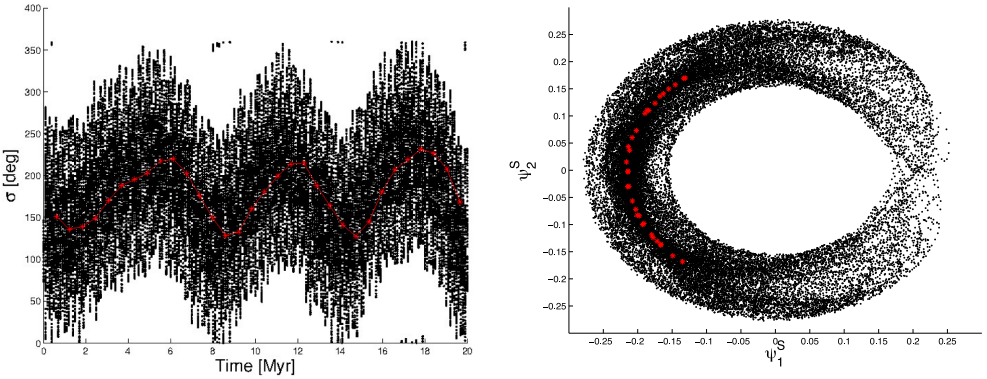

Figure 3. Panel A: the time evolution of the resonance argument $\sigma = 2(\varpi - \varpi_6) + (\Omega - \Omega_6)$ (black dots). The red asterisks show the argument after being digitally filtered so as to remove all frequencies corresponding to periods less than 700 000 yr. Panel B: orbital evolution in the polar plane (${\psi_1}^S$, ${\psi_2}^S$). The resonant elements (${\psi_1}^S$, ${\psi_2}^S$) were also digitally filtered with the same procedure (red asterisks).

4 COMPOSITIONAL ANALYSIS: TAXONOMY AND PHYSICAL PROPERTIES

Only five objects had taxonomical data in three major photometric/spectroscopic surveys (ECAS (Eight-Colour Asteroid Analysis; Zellner, Tholen & Tedesco 1985; Tholen 1989), SMASS (Small Main Belt Spectroscopic Survey; Xu et al. 1995; Bus & Binzel 2002a, Bus & Binzel2002b), and S3OS2 (Small Solar system Objects Spectroscopic Survey; Lazzaro et al. 2004): 60 Echo (S-type), 163 Erigone (C), 571 Dulcinea(S), 2763 Jeans (V), and 2991 Bilbo (C). Using the classification method of De Meo & Carry (2013) that employs Sloan Digital Sky Survey-Moving Object Catalog data, fourth release (SDSS-MOC4 hereafter; Ivezić et al. 2001) to compute *gri* slope and $z' - i'$ colours, we obtained a set of 470 observations of asteroids (including multiple observations of the same object) in the Erigone region. This corresponds to 276 asteroids for which an SDSS-MOC4 taxonomical classification and proper elements are both available. We found 30 X, 7 D, 103 C, 52 L, 66 S, 3 V, and 5 B type objects, respectively. There were data for 18 objects currently inside the z_2 secular resonance, 6 were L-, 4 S-, 4 C-, 2 K-, and 2 B-types.

Fig. 4, panel A, displays a projection in the *gri* slope versus $z' - i'$ plane for the 276 observations in the SDSS-MOC4 catalogue for asteroids in the Erigone region, while panel B shows an (a, $\sin(i)$) projection of asteroids in the same region. As in Carruba et al. (2013), that, however, used a simplified method allowing only to distinguish if an asteroid belonged to the C-complex, S-complex, or was a V-type, we found that the Erigone region is dominated by the C-type Erigone family, but with significant mixing of other S- and V-type objects.

Concerning albedo information, we identified 1053 asteroids with *WISE* albedo information (Masiero et al. 2012) in the Erigone region. Our analysis confirms that of Carruba et al. (2013): the Erigone region has a predominance of lower albedos, with 802 asteroids (76.2 per cent of the total) with $p_V < 0.15$, associated with C-complex objects, and 251 (23.84 per cent of the total) bodies with $p_V > 0.15$, associated with S-complex and V-type objects.[3] Using the values of the diameters from *WISE*, when available (otherwise diameters are estimated using absolute magnitudes and the mean value of geometric albedo in the Erigone region, i.e. $p_V = 0.033$ via equation 4 in Carruba et al. 2003), and the density of 163 Erigone from Carry (2012), we computed the masses of asteroids in the Erigone region, assumed as homogeneous spheres. For the few asteroids where an estimate of the mass was reported in Carry (2012), we used the values from that paper. The only two objects with a mass larger than 10^{17} kg in the region are 163 Erigone itself, and the family-less S-type 60 Echo. This would suggest that the only large C-type family in the region should be the one associated with 163 Erigone. We will further investigate this issue in the next section.

5 FAMILY IDENTIFICATION

To obtain family membership of the Erigone family (FIN 406, according to Nesvorný, Broz & Carruba 2015), we first followed the approach of Carruba et al. (2015), where the hierarchical clustering method was used in a domain of proper elements (a, e, $sin(i)$) and *gri* slope and $z' - i'$ colours from SDSS-MOC4, in the restricted sample (280 asteroids, 5.94 per cent of the 4717 asteroids in the area), for which this information is available. While the sample of asteroids in this domain is reduced, this method is more efficient in eliminating possible interlopers then standard HCM in the domain of proper (a, e, $\sin(i)$) only, and can provide clues about the possible existence (or not) of large families in the area. The value of the minimal distance cut-off d_0 defined as in Beaugé & Roig (2001) was of 154.5 m s^{-1} and the minimal number of objects to have a group statistically significant was 25. In this five-dimension domain the Erigone family merged with the local background for a cut-off of 225 m s^{-1}, and we did not find any other significant groups in the region, so confirming the hints provided by the analysis of asteroid masses in the region in the previous section. Following Spoto et al. (2015), we considered the groups around 163 Erigone and 5026 Martes as belonging to the same dynamical family.

We then used a standard HCM approach in the (a, e, $sin(i)$) domain, with the methods described in Bendjoya & Zappalà (2002) for the 4717 asteroids with synthetic proper elements in the area. As in Carruba et al. (2013), we decided to work with a family obtained

[3] The boundary between C- and S-complex classes in albedo varies in the literature. While most of C-type objects have values of albedos less than 0.1, recent results from *WISE* showed that some C-type families, such as 2782 Leonidas, 1128 Astrid, and 18405 FY12, have significant tails at higher albedos than previously thought. Also, *WISE* albedo data has usually errors of the order of 10 per cent, 20 per cent for $p_V \simeq 0.1$. In this work, we prefer to exclude less objects by using a higher threshold ($p_V = 0.15$), rather than run the risk of eliminating possible family members.

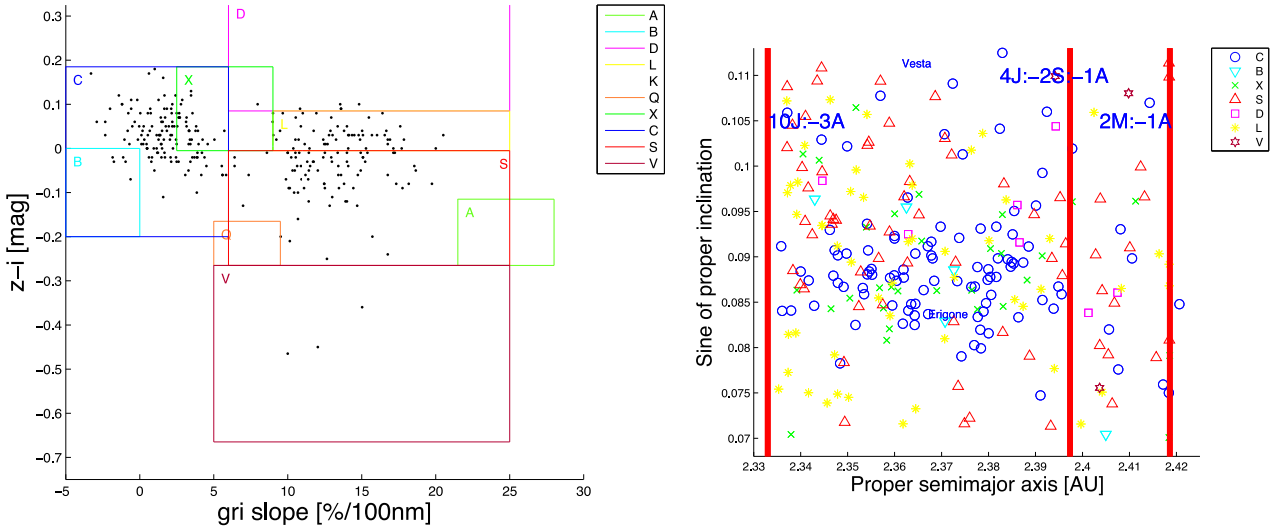

Figure 4. Panel A: a projection in the *gri* slope versus $z' - i'$ plane of the 276 observations in the SDSS-MOC4 catalogue for asteroids in the Erigone region. Panel B: an $(a, \sin(i))$ projection of the 280 asteroids with taxonomical information in the same area.

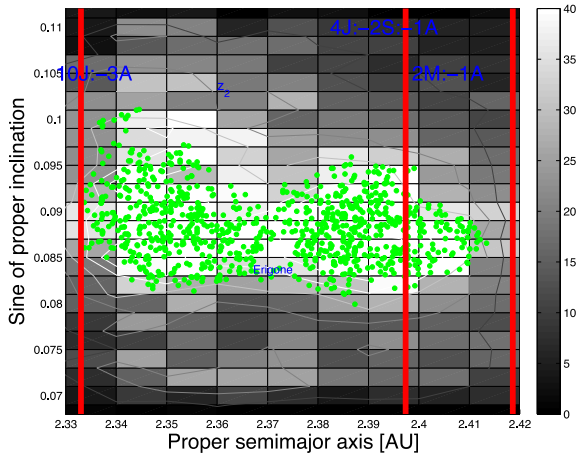

Figure 5. Contour plot of number density of asteroids in the same region. Green dots show the location of members of the identified Erigone family.

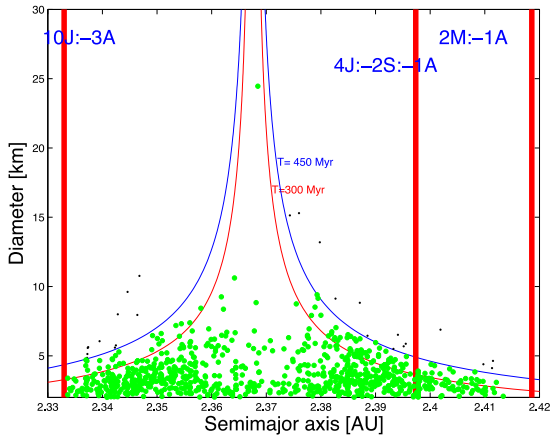

Figure 6. A proper a versus diameter projection of members of the Erigone family. The red and blue curves display isolines of maximum displacement in a caused by Yarkovsky effect after 300 Myr (red line) and 450 Myr (blue line). Green full dots are associated with Erigone family members, black dots display the location of dynamical interlopers.

at a cut-off of 40 m s^{-1}. After eliminating nine asteroids with incompatible taxonomy, and eight objects with albedo $p_V > 0.15$, we were left with a family of 880 members. Fig. 5 displays a contour plot of number density of asteroids in the Erigone region, where green full dots identify the orbital location of the family members identified in this work. We plotted a contour plot of the number density of background asteroids, rather than showing the location of each asteroid orbit as a dot, so as to facilitate the visual identification of the Erigone family members. We computed the number of asteroids per unit square in a 30 by 30 grid in the $(a, \sin(i))$ plane, with a between 2.3 and 2.45 and $sin(i)$ between 0.065 and 0.95. Regions with lower number of asteroids are usually (but not always) associated with dynamically unstable region. Number density of asteroids may therefore provide clues about the local dynamics. As discussed before, no other significant group was identified in the Erigone area.

We identified 123 members of the Erigone dynamical family in librating states of the z_2 secular resonance, but only five members in $3\nu_6 - \nu_5$ librating states, and none in $\nu_5 + 2\nu_{16}$ librating states. Because of the very low numbers of resonant objects (less then 0.6 per cent of the $(a, e, sin(i))$ family at most), no statistically significant information can be unfortunately derived from an analysis of the dynamical evolution of the resonant populations of the latter two resonances.

As a next step in our research, we then obtained a preliminary estimate of the age of the families and attempted to eliminate possible dynamical interlopers using the method of Yarkovsky isolines. Following the approach of Carruba et al. (2015), we computed isolines of displacements caused by the Yarkovsky effect for a C-type family. Dynamical interlopers are objects that reside beyond the maximum possible Yarkovsky isoline, and could not have reached their current orbital position since the family formation. Fig. 6 displays the results of our method. Overall, we found 26 asteroids that could be classified as dynamical interlopers, leaving us with a family of 854 objects.

In the next section, we will use the so-called Yarko-YORP Monte Carlo method of Vokrouhlický et al. (2006a,b,c), modified to account for new developments in our understanding of the YORP

effect, to try to refine the preliminary estimates of the family age obtained in this section.

6 CHRONOLOGY

Monte Carlo methods to obtain estimates of the family age and ejection velocity parameters were pioneered by Milani & Farinella (1994) and improved by Vokrouhlický et al. (2006a,b,c) for the Eos and other asteroid groups. They were recently modified to account for the 'stochastic' version of the YORP effect (Bottke et al. 2015), and for changes in the past values of Solar luminosity (Vokrouhlický et al. 2006a) for a study of dynamical groups in the Cybele region (Carruba et al. 2015). We refer the reader to the latter paper for a more in depth description of the method. Essentially, the semimajor axis distribution of various fictitious families is evolved under the influence of the Yarkovsky, both diurnal and seasonal versions, and YORP effect (and occasionally other effects such as close encounters with massive asteroids (Carruba, Aljbaae & Souami 2014) or changes in past solar luminosity values (Carruba et al. 2015). The newly obtained distributions of a C-target function are computed with the relationship:

$$0.2H = \log_{10}(\Delta a/C), \tag{3}$$

where H is the asteroid absolute magnitude. We applied this method to the Erigone group obtained in Section 5. Fig. 7 displays $\psi_{\Delta C}$ values in the (Age, V_{EJ}) plane for this family. Values of the V_{EJ} parameter have to be lower than the estimated escape velocity from the parent body (Bottke et al. 2015), 59.2 m s^{-1} for the case of the Erigone family. Using $\psi_{\Delta C} = 9.4$ (red line in Fig. 7), corresponding at a confidence level of 81.2 per cent to the two distribution being compatible (Press et al. 2001, there were 12 intervals in the C distribution), the Erigone family should be 190^{+50}_{-40} Myr old, with $V_{EJ} = 55^{+5}_{-30}$ m s^{-1}. As discussed in the introduction, Vokrouhlický et al. (2006c) used a Yarko-Yorp approach to find an age of 280^{+30}_{-50} Myr. The slightly smaller value found in this work could be caused by the fact that we are including the stochastic version of the YORP effect. Our estimate seems to be more in agreement with that of Bottke et al. (2015), 170^{+25}_{-30} Myr, that included this effect, and with the age estimate of Spoto et al. (2015), who found an age of 220^{+60}_{-80} Myr with an independent method.[4] Overall, there seems to be a consensus in the literature that the Erigone family should be a relatively young C-type cratering family.

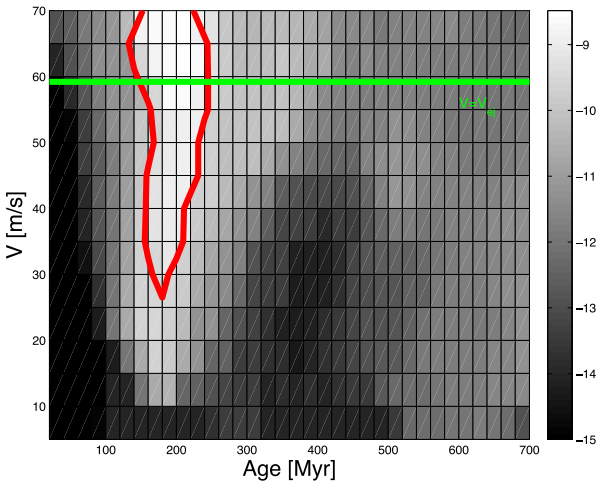

Figure 7. Target function $\psi_{\Delta C}$ values in the (Age, V_{EJ}) plane for Erigone family. The horizontal green line displays the value of the estimated escape velocity from the parent body.

In the next section, we will study the constraints that can be put on the Erigone family age by dynamics inside the z_2 secular resonance.

7 DYNAMICS INSIDE THE z_2 SECULAR RESONANCE

About 14.4 per cent of the members of the Erigone family identified in the (a, e, $sin(i)$) domain are currently in librating states of the z_2 secular resonance. While well below 50 per cent of the family membership, there is still quite a significant population of Erigone members in librating states to allow us to infer some constraints on the dynamical evolution and age of the Erigone group.

First, we analysed the current dispersion of librating asteroids in the plane (σ, $\frac{d\sigma}{dt}$), where σ is the z_2 resonant argument $2(\varpi - \varpi_6) + (\Omega - \Omega_6)$, and $\frac{d\sigma}{dt}$ is the associated frequency $2(g - g_6) + (s - s_6)$. The procedure followed to compute the quantities in Fig. 8, panel A is as follows. The orbital elements results of the numerical simulation over 30 Myr are used to obtain equinoctial, non-singular element of the form ($e \cdot \cos \varpi$, $e \cdot \sin \varpi$), and ($\sin(i/2)\cos \Omega$, $\sin(i/2)\sin \Omega$). The equinoctial elements of the test particles and of Saturn are then Fourier filtered to obtain the g, s, g_6, s_6 frequencies and their associated phases. The frequencies are then plotted on the ordinates and their phases are used to construct the resonant angle σ, for the 92 objects that remained in librating states for the whole length of the simulation.

The reader may notice in Fig. 8, panel A, that no resonant asteroid was found at values of $2(g - g_6) + (s - s_6)$ greater than 0.3 arcsec yr^{-1} or lower then -0.3 arcsec yr^{-1}, so confirming the criteria of Carruba (2009) used in Section 3. One can also notice that, as for the case of the ν_6 (Carruba & Morbidelli 2011) and z_1 resonances (Vokrouhlický et al. 2006b; Carruba 2009), there is an equilibrium point at $\sigma = 180°$. Contrary to the cases of the ν_6 and z_1, data has a poor signal-to-noise ratio and is difficult to interpret. The resonant behaviour of a single particle will be better displayed later on in this section (see Fig. 9).

Fig. 8, panel B, deals with conserved quantities of the z_2 secular resonance. It is possible to show (see Carruba & Morbidelli 2011; Vokrouhlický et al. 2006b; Carruba 2009, and calculations therein) that $K_2' = \sqrt{1-e^2}(1 - \cos i)$ is conserved for the ν_6 resonance, $K_2' = \sqrt{1-e^2}(2 - \cos i)$ is preserved for the z_1 resonance, and $K_2' = \sqrt{1-e^2}(3 - \cos i)$ is conserved for the z_2 one. Fig. 8, panel B, displays normalized distributions of the quasi-integral K_2' for the (a, e, i) (black line), and (n, g, $2g + s$) (green line) groups. Since less than 50 per cent of the Erigone members are in z_2 librating states, we cannot use the conservation of this quantity to set constraints on the original ejection velocity field, as done for the Tina, Agnia and Padua family. Yet, checking its behaviour as a function of time, may show how well this quantity is actually preserved for the z_2 resonance, and if it could be possibly used for other z_2 resonant groups, should they ever be discovered.

To further investigate dynamics inside the z_2 resonance we devised this numerical experiment: we started with a synthetic Erigone family as a tightly compact cluster in a, e, $sin(i)$ and σ. This family is initially a compact cloud as shown in the first panel of Fig. 9. To

[4] In Spoto et al. (2015), the Erigone family is considered as the merger of the Erigone family and the 5026 Martes group.

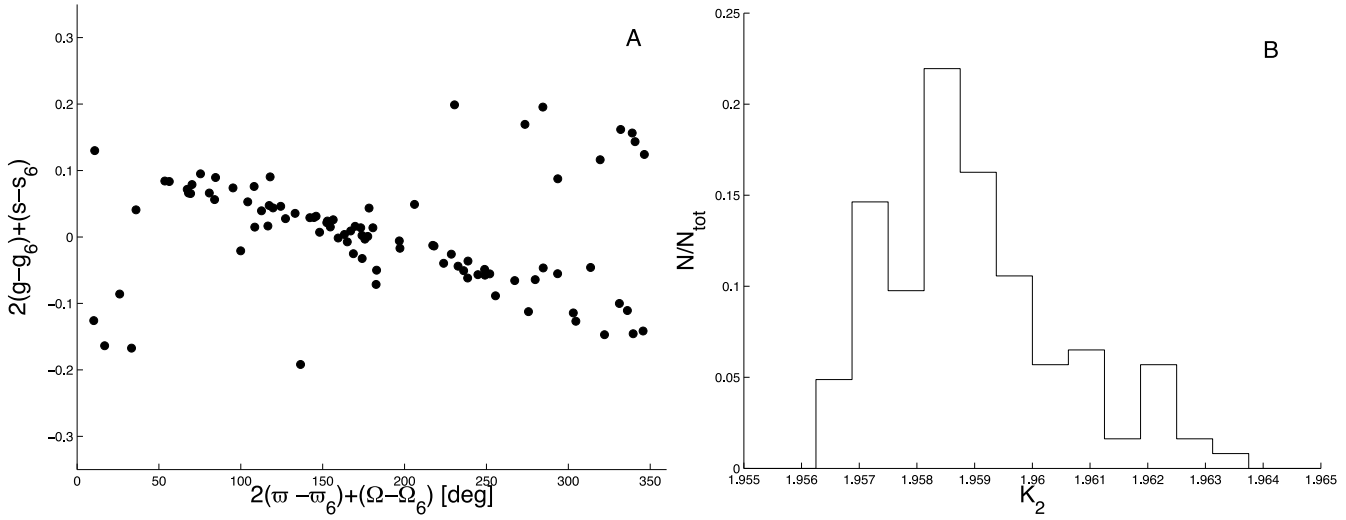

Figure 8. Panel A: z_2 librating members of the (a, e, i) (full black dots) Erigone family, displayed in a plane where the x-axis is the z_2 resonant argument $2(\varpi - \varpi_6) + (\Omega - \Omega_6)$ and the y-axis is the associated frequency $2(g - g_6) + (s - s_6)$. Panel B: normalized distribution of the quasi-integral $K_2{}' = \sqrt{1-e^2}(3 - \cos(i))$ values for the Erigone (a, e, i) (black line) members currently inside the z_2 resonance.

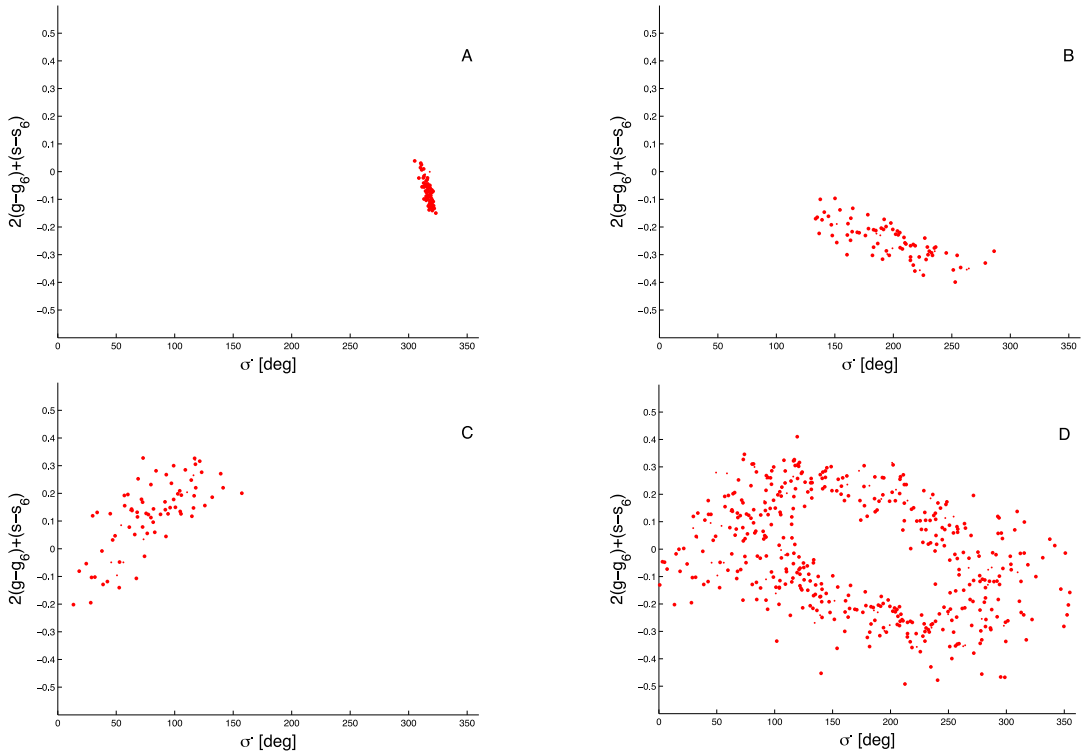

Figure 9. Snapshots of the numerically integrated evolution of clones of Erigone family member 8089 Yukar (red dots) projected on to the z_2 resonance variables: the state after t = 1.2 Myr (panel A), after 3.7 Myr (panel B), after 6.1 Myr (panel C), and all data points between 3.7 and 9.8 Myr, panel D).

better define the time it takes for the cloud to disperse, the fake family is composed by 81 'clones' produced by adding and subtracting small values to the eccentricity (0.0001) and inclination (0.001) of 8089 Yukar, the lowest numbered asteroid in our sample in a z_2 librating state.

Fig. 9 shows the evolution of the synthetic family as tracked in the space of the z_2 resonance variables (σ, $\mathrm{d}\sigma/\mathrm{d}t$). The last panel show all data points between 3.7 and 9.8 Myr, a period that covers an entire z_2 libration cycle. After $\simeq$ 12.3 Myr, the initially tight cluster becomes uniformly dispersed along the separatrix of the z_2 resonance. Notice that, contrary to the cases of the ν_6 and z_1 secular resonances, while the period of libration remains approximately constant, the amplitude changes in a chaotic fashion. After a few libration cycles, particles with very close initial conditions may find themselves quite apart in the (σ, $\mathrm{d}\sigma/\mathrm{d}t$) plane, as indeed observed in Fig. 8, panel A. To quantitatively describe the distribution of

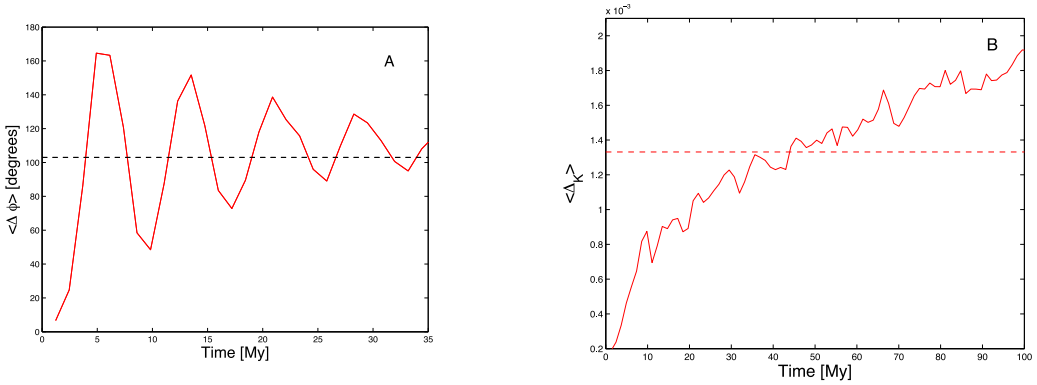

Figure 10. Panel A: temporal evolution of D^2_Φ of equation (4) for the synthetic Erigone family. Panel B: temporal evolution of D_K, dispersion of the $K_2^{'}$ variable. The dotted line displays the mean value of D_K during the simulation.

bodies along the z_2 separatrix, we used the polar angle Φ in the (σ, dσ/dt) plane described in Vokhrouhlický et al. (2006b).[5] At each step of the numerical simulation, we computed the dispersion $D;_\Phi$ in the polar angle Φ defined as

$$D^2_\Phi = \frac{1}{N(N-1)} \sum_{i \neq j} (\Phi_i - \Phi_j)^2, \quad (4)$$

where $N = 81$ is the number of integrated bodies and Φ_i is the polar angle of the ith body (i = 1,...,N). Since we started with a compact cluster, D^2_Φ is initially small ($\simeq 6.^\circ 61$), but grows with time because of the differential libration of the bodies in the resonance (Fig. 10, panel A). After only $\simeq$ 12 Myr, i.e. about two libration cycles of the z_2 resonance for (8089) Yukar, the value of D^2_Φ saturates at $\simeq 103^\circ$, which corresponds to an uniform distribution of bodies along a circle (Vokrouhlický et al. 2006b). This result suggests that any information about initial distributions of orbits inside the z_2 resonance is lost very quickly, on a time-scale of the order of 10 Myr.

Fig. 10, panel B, displays the time evolution of the dispersion D_K of the $K_2^{'}$ quantity. Contrary to the case of the z_1 resonance, where D_K was nearly constant over the entire integration time span of 100 Myr and perturbations occurred only when some of the bodies left the z_1 resonance, here perturbations of the $K_2^{'}$ are quite significant. The percentual change in D_K, defined as the standard deviation of D_K divided by its averaged value, was 30.1 per cent. Results are similar when non-gravitational forces such as the Yarkovsky and YORP effects are considered, and will not be here discussed for the sake of brevity. This result shows that it is not easily feasible to use the observed $K_2^{'}$ distribution to infer quantitative information about the initial velocity field, as done for instance for families inside the z_1 resonance, such as the Agnia and Padua groups. This is not a big issue for the Erigone family, since the majority of its members are not currently in z_2 librating states, but is a fact to be considered if a dynamical group with a majority of its members in such configuration will be discovered in the future.

The next section will deal with the dynamical evolution of the Erigone family as whole, and on what constraints can be set by studying its interaction with the z_2 secular resonance.

[5] We used a scaling that maps a (0°, 360°) interval of σ and (−1,1) arcsec yr^{-1} interval in dσ/d$t = g + s - g_6 - s_6$ into common intervals (−1,1).

8 DYNAMICAL EVOLUTION OF THE ERIGONE FAMILY

To study the dynamical evolution of the Erigone family members, we performed simulations with the *SYSYCE* integrator (Swift+Yarkovsky+Stochastic YORP+Close encounters) of Carruba et al. (2015), modified to also account for past changes in the values of the solar luminosity. The numerical setup of our simulations was similar to the one discussed in Carruba et al. (2015): we used the optimal values of the Yarkovsky parameters discussed in Brož et al. (2013) for C-type asteroids, the initial spin obliquity was random, and normal reorientation time-scales due to possible collisions as described in Brož (1999) were considered for all runs. We integrated our test particles under the influence of all planets, and obtained synthetic proper elements with the approach described in Carruba (2010).

We generated a fictitious family of 854 objects with the ejection parameter V_{EJ} found in Section 6, and integrated this group over 400 Myr, well beyond the maximum possible value of the age of the Erigone family. We then analysed the resonant argument σ of the z_2 secular resonance for all simulated particles. The behaviour of this angle could be quite complex: because of the drift in semi-major axis caused by non-gravitational forces, asteroids can be temporarily captured in the z_2 resonance, then escape to circulating orbits, then, should the direction of the drift change, be captured again, etc. Fig. 11 displays the time dependence of the z_2 resonant argument of a simulated particle that alternated between phases of libration and circulation in the z_2 secular resonance. Overall, while the number of z_2 librators should change with time, if the population of librators from the Erigone family is in a steady-state, this number should fluctuate around the median value, with fluctuation of the order of one standard deviation. Similar behaviour is for instance observed for the population of asteroids currently inside the M2:1A mean-motion resonance (Gallardo et al. 2011). The minimum time needed to reach a steady-state could therefore be used to set constraints on the age of the Erigone family.

We analysed the resonant angle of all simulated particles, and computed the fraction of family members in z_2 resonant states as a function of time. Fig. 12 displays our results: the number of z_2 librators fluctuates with time, but reaches its median value after 125 Myr (after $\simeq$ 90 Myr if we consider the median value plus or minus the standard deviations as an estimate of the error, blue dashed lines in Fig. 12). We believe that this result is of quite significance, since (i) sets a lower limit on the age of the Erigone family, that is compatible with this family age estimates obtained in

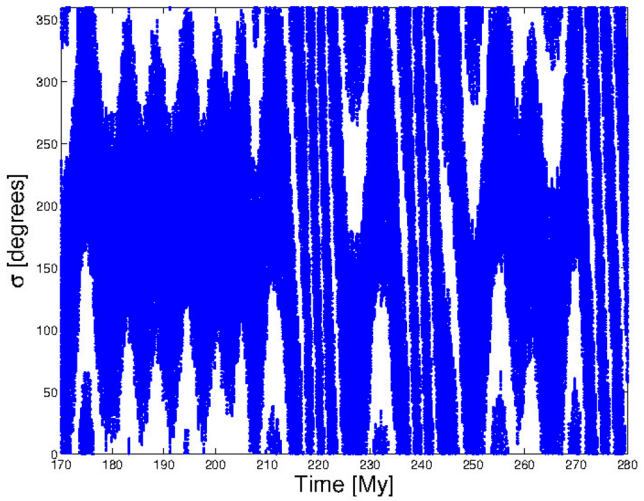

Figure 11. Time behaviour of the z_2 resonant argument of a simulated particle between 170 and 280 Myr.

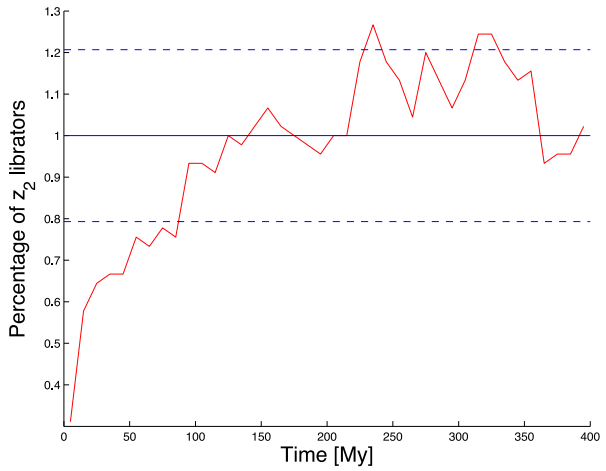

Figure 12. Fraction of simulated Erigone family members in z_2 librating states as a function of time, normalized with respect to the median value. The horizontal blue line displays the median percentage of objects in the z_2 states, dashed lines display levels of median fraction plus or minus its standard deviation.

this and other works, and, (ii) most importantly, is obtained using a new technique, purely based on secular dynamics, not previously used in the literature.

9 CONCLUSIONS

In this work, we:

(i) Computed proper elements for a dynamical map and real asteroids in the Erigone family region. The Erigone family is characterized by its interaction with the z_2 secular resonance, and we found synthetic proper elements for 4717 asteroids.

(ii) Studied the local secular dynamics. There are 367 asteroids currently in z_2 librating states. Other important non-linear secular resonances in the area are the $3\nu_6 - \nu_5$, a g −type resonance, with 75 librators, and the $\nu_5 + 2\nu_{16}$, a $(g + 2s)$ −type resonance, with 38 librators.

(iii) Revised current knowledge on the taxonomy and physical properties of local asteroids. The Erigone region is dominated by the C-type Erigone family, but with significant mixing of other S- and V-type objects. Except for the family-less S-type 60 Echo, the only other object with a mass larger than 10^{17}kg in the region is 163 Erigone itself, with other bodies being most likely either members of the Erigone or of other families.

(iv) Identified the Erigone family in the domain of proper (a, e, $sin(i)$) elements and proper (n, g, $g + s$) and (n, g, $2g + s$) frequencies, the latter domain being the most efficient in identifying objects in z_2 librating states. After eliminating taxonomical and dynamical interlopers, we obtained an (a, e, $sin(i)$) family of 854 members, 14.4 per cent of which in z_2 librating states.

(v) Obtained estimates of the Erigone family age with a Yarko-Yorp Monte Carlo method that also accounts for the 'stochastic' version of the YORP effect, and for changes in the past values of Solar luminosity (Carruba et al. 2015). At a 81.2 per cent confidence level, the Erigone family should be 190^{+50}_{-40} Myr old, with $V_{EJ} = 55^{+5}_{-30}$ m s^{-1}. Results are in agreement with those of other groups (Vokrouhlický et al. 2006c; Bottke et al. 2015; Spoto et al. 2015).

(vi) Studied the dynamics inside the z_2 secular resonance. We observe one stable equilibrium point at $\sigma = 180^\circ$ in the z_2 resonance plane (σ, $\frac{d\sigma}{dt}$), with $\sigma = 2(\varpi - \varpi_6) + (\Omega - \Omega_6)$ the resonant angle of the z_2 resonance. Current members of the (a, e, $sin(i)$) and (n, g, $2g + s$) Erigone families are fully dispersed around the equilibrium point. Since the minimum time to achieve such configuration is $\simeq$ 12 Myr, this sets a lower limit on the Erigone family age.

(vii) Studied the dynamics of the Erigone family as a whole, and showed that the minimum time to inject into z_2 librating states a steady-state population is 90 Myr, which sets another constraint on the family age.

Overall, our estimate of the Erigone family age is compatible with values in the literature. More important, by studying the very interesting dynamics inside the z_2 secular resonance, we were able to set two additional independent lower limits to the family age. These new tools based on secular dynamics of a resonant family constitute, in our opinion, one of the main results of this work.

ACKNOWLEDGEMENTS

We are grateful to an anonymous reviewer for comments and suggestion that improved the quality of this paper. This paper was written while VC was a visiting scientist at the SouthWest Research Institute (SWRI) in Boulder, CO, USA. We would like to thank the São Paulo State Science Foundation (FAPESP) that supported this work via the grants 14/24071-7, 14/06762-2, 2013/15357-1, and 2011/08171-3, and the Brazilian National Research Council (CNPq, grants 312313/2014-4 and 312813/2013-9). This publication makes use of data products from the *Wide-field Infrared Survey Explorer*, which is a joint project of the University of California, Los Angeles, and the Jet Propulsion Laboratory/California Institute of Technology, funded by the National Aeronautics and Space Administration. This publication also makes use of data products from NEOWISE, which is a project of the Jet Propulsion Laboratory/California Institute of Technology, funded by the Planetary Science Division of the National Aeronautics and Space Administration.

REFERENCES

Beaugé C., Roig F., 2001, Icarus, 153, 391
Bendjoya P., Zappalà V., 2002. Asteroids III, Univ. Arizona Press, Tucson, AZ, p. 613
Bottke W. F. et al., 2015, Icarus, 247, 191

Brož M., 1999, Thesis, Charles Univ., Prague
Brož M., Morbidelli A., Bottke W. F., Rozenhal J., Vokrouhlický D., Nesvorný D., 2013, A&A, 551, A117
Bus J. S., Binzel R. P., 2002a, Icarus, 158, 106
Bus J. S., Binzel R. P., 2002b, Icarus, 158, 146
Carruba V., 2009, MNRAS, 395, 358
Carruba V., 2010, MNRAS, 408, 580
Carruba V., Michtchenko T. A., 2007, A&A, 475, 1145
Carruba V., Michtchenko T. A., 2009, A&A, 493, 267
Carruba V., Morbidelli A., 2011, MNRAS, 412, 2040
Carruba V., Burns J. A., Bottke W., Nesvorný D., 2003, Icarus, 162, 308
Carruba V., Michtchenko T. A., Roig F. Ferraz-Mello S., Nesvorný D., 2005, A&A, 441, 819
Carruba V., Domingos R. C., Nesvorný D., Roig F., Huaman M. E., Souami D., 2013, MNRAS, 433, 2075
Carruba V., Aljbaae S., Souami D., 2014, ApJ, 792, 46
Carruba V., Nesvorný D., Aljbaae S., Domingos R. C., Huaman M. E., 2015, MNRAS, 451, 4763
Carry B., 2012, Planet. Space Sci., 73, 98
Charlier C. V. L., 1902, Die Mechanik des Himmels. Verlag Von Veit, Leipzig
De Meo F., Carry B., 2013, Icarus, 226, 723
Gallardo T., Venturini J., Roig F., Gil-Hutton R., 2011, Icarus, 214, 632
Ivezić Ž. et al., 2001, AJ, 122, 2749
Knežević Z., Milani A., 2003, A&A, 403, 1165
Lazzaro D., Angeli C. A., Carvano J. M., Mothé-Diniz T., Duffard R., Florczak M., 2004, Icarus, 172, 179
Masiero J. R., Mainzer A. K., Grav T., Bauer J. M., Jedicke R., 2012, ApJ, 759, 14
Milani A., Farinella P., 1994, Nature, 370, 40
Milani A., Knežević Z., 1990, Celest. Mech. Dyn. Astron., 49, 347
Milani A., Knežević Z., 1994, Icarus, 107, 219
Nesvorný D., Broz M., Carruba V., 2015, Identification and Dynamical Properties of Asteroid Families, preprint (arXiv:1502.01628)
Press V. H., Teukolsky S. A., Vetterlink W. T., Flannery B. P., 2001, Numerical Recipes in Fortran 77. Cambridge Univ. Press, Cambridge, p. 209
Spoto F., Milani A., Knežević Z., 2015, Icarus, 257, 275
Tholen D. J., 1989, in Binzel R. P., Gehrels T., Matthews M. S., eds, Asteroid Taxonomic Classifications, Univ. Arizona Press, Tucson, AZ, p. 298
Vokrouhlický D., Brož M., Morbidelli A., Bottke W. F., Nesvorný D., Lazzaro D., Rivkin A. S., 2006a, Icarus, 182, 92
Vokrouhlický D., Brož M., Bottke W. F., Nesvorný D., Morbidelli A., 2006b, Icarus, 182, 118
Vokrouhlický D., Brož M., Bottke W. F., Nesvorný D., Morbidelli A., 2006c, Icarus, 183, 349
Xu S., Binzel R. P., Burbine T. H., Bus S. J., 1995, Icarus, 115, 1
Zellner B., Tholen D. J., Tedesco E. F., 1985, Icarus, 61, 355

This paper has been typeset from a TEX/LATEX file prepared by the author.